

Adaptive digital MPPT control for photovoltaic applications.

C. Cabal¹, C. Alonso¹, A. Cid-Pastor², B. Estibals¹, L. Segulier¹, R. Leyva², G. Schweitz³, J. Alzieu³

¹University of Toulouse
LAAS-CNRS

7 Avenue du Colonel Roche
31 077 Toulouse Cedex 04 FRANCE
ccabal@laas.fr, alonsoc@laas.fr

²University of Rovira I Virgili
D.E.E.A

26 Av. Dels Països Catalans
43 007 Tarragona ESPAGNE
Angel.cid@urv.cat

³EDF

Electrical Equipment Laboratory
Les Renardières
77 818 Moret sur Loing FRANCE
Guy.schweitz@edf.fr

SS3 : Power Electronics for Photovoltaics

Abstract – Maximum Power Point Tracker (MPPT) is often used to increase the energy conversion efficiency for intermittent energy sources. Numerous of research teams work today to improve this type of algorithms. We had developed real-time MPPT controls based on the Extremum Seeking Control principle first implemented on analogical circuit. Today, to be more flexible and adaptive with several structures of power static converters, our new MPPT algorithms are implemented on numerical circuits. Our aim is to obtain high performances. To achieve a high quality matching between sources and loads, our new MPPT control adjusts continually the static converter duty cycle. Transitory effects are immediately detected and new MPP rapidly recovered. In addition, this digital control has an adjustment delay which allows an adaptation to a large power range from high to low points and then a real optimisation. Experimental results validate the global behaviour of this control for photovoltaic systems.

I. INTRODUCTION

To protect the environment from the industrial pollution and the greenhouse effect, several research and development projects have been realised on renewable energy. Indeed, the potential of these energies is focused on their abundance all over the world and their clean treatment. For the solar energy use, the actual drawback stays its high cost. This problem can be resolved through different improvements in term of energy production. For that, different axis of researches can be explored. In fact, a photovoltaic (PV) cells must be improve in their performances and reduction cost. We focused our effort to improve the matching between PV sources and loads through the development of new performing and small elementary conversion chains (i.e. small static converters able to accept MPPT controls). Converters are chosen having high conversion efficiencies and able to be connected in series and/or parallel to feet a large power domain. In parallel, we focused our work on an improvement of matching with a permanent extraction of maximum power electrical energy from solar generators through MPPT algorithms. Indeed, to obtain permanently the maximum power of intermittent sources, a perfect matching must be done between the internal source impedances and loads. The classical solution consists to introduce an adaptation stage between the panel and the load (a static converter) associated with a MPPT working as an impedance matching.

Different types of MPPT exist. Their differences depend of the type of implementation, the theoretical control principle and the acquisition parameters. Indeed, this function of control may be realised with analogical or digital implementation. The number of sensors varies function of precision researched. It may be one or more of the input and/or the output parameters of the static power converter. The principle of the control may be established from the mathematical model [1, 2] or using Perturb and Observation algorithm [3-9]. All of them attempt to obtain the maximal power point more or less successfully, and have the solar variation dynamic behaviour more or less acceptable.

Since 2000, different versions of MPPT based on Extremum Seeking Control principle had been created [3, 4, and 9]. This paper presents the last version of the digital implementation designed in our laboratory. It was validate for photovoltaic systems and was able to track the optimal PV power point in all of working cases. The control was designed to be implemented through a microcontroller PIC 18F1220 and work with a permanent modification of the duty cycle value delivered to a converter to obtain a high matching. An additional function is integrated in the digital algorithm to improve the efficiency of the MPPT and the PV power production whatever the irradiation level resolving the problems of majority of MPPT which present low efficiency for low irradiations.

In section II, the photovoltaic module characteristics are discussed, justifying the utilization of an MPPT control. Section III describes the theory of Extremum Seeking Control principle. In part IV, the digital MPPT algorithm is explained. Experimental results for different operating conditions are shown in Section V. Finally, conclusions are presented in section VI.

II. CHARACTERISTICS OF THE SOLAR PANEL

A photovoltaic sensor is based on the physical phenomenon called “photovoltaic effect”. The principle consists to transform the photons emitted by the sun in electrical energy. The equivalent circuit of PV solar cell is illustrated on the Fig. 1.

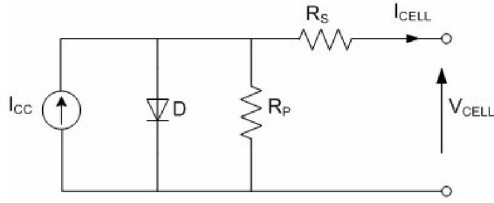


Fig. 1. Static model circuit of PV solar panel.

The output current of a cell is function of the insulation and the temperature, given by the equation below:

$$I_{CELL} = I_{CC} - I_{SAT} \left[\exp\left(\frac{V_{CELL} + I_{CELL} R_S}{nV_T}\right) - 1 \right] - \frac{V_{CELL} + I_{CELL} R_S}{R_P} \quad (1)$$

$$\text{with } V_T = \frac{KT}{e}$$

In the equation (1), I_{SAT} is the saturation current, V_T is the thermodynamics potential, K the Boltzmann's constant, T the cell temperature formulated in Kelvin, e the electron charge, n the idealistic factor for a p-n junction. Respectively I_{CELL} and V_{CELL} are the output current and voltage of the panel, I_{CC} the panel short-circuit current depending of the insulation and the temperature, R_P the shunt resistance which characterised the leakage current of the junction and R_S the series resistance which represented the different contact and connection resistances.

Even, the power delivered by one cell is not enough to supply a load. For medium and high power applications, it is necessary to use several PV cells connected in series/parallel to form a photovoltaic array and reach a desired power.

According to (1), static electrical characteristics $I(V)$ of the photovoltaic array is non linear. The panel characteristics (Fig.2) can be assimilated to a current source on the left of the optimal point or to a voltage one on the right of the optimal point. At the Maximum Power Point (MPP), the PV behaviour can be considered like a power source and is characterised by an optimal current and voltage (I_{OPT} , V_{OPT}).

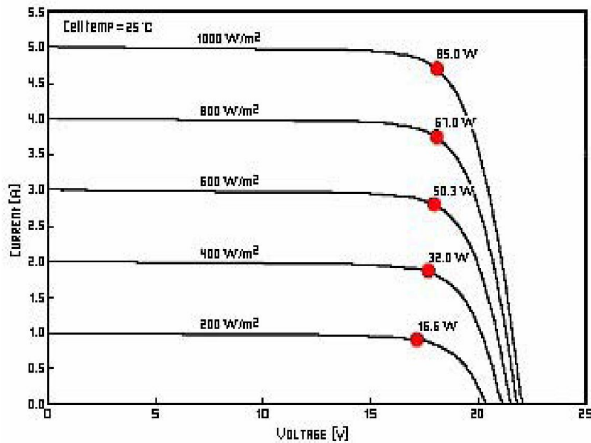


Fig. 2. $I_{PV}(V_{PV})$ static characteristics of a solar panel BP 585 at 25°C function of solar irradiances.

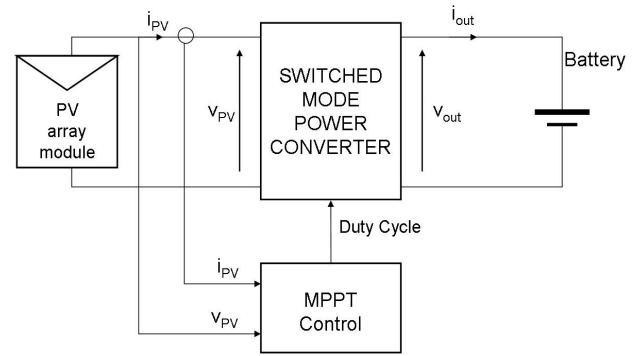


Fig. 3. MPPT control block adapted to a PV conversion chain.

This MPP varies according to the sun irradiation and ambient temperature (Fig.2). The maximum power is transferred to the load when the impedance source matches the load one. To accomplish this objective, a switching converter is placed between the PV source and the load (Fig. 3). With a MPPT control it is possible to reach the output panel characteristics around the optimal voltage (V_{OPT}) for extract the maximum energy.

III. EXTREMUM SEEKING CONTROL PRINCIPLE

In a previous work of R. Leyva [4], the stability of the Extremum Seeking algorithm was demonstrated. The theoretical and experimental analyses were realised with a Boost converter. This structure is used as a matching stage (Fig 3). The different blocks of this MPPT method are depicted in Fig.4. The equations describing the system behaviour are composed by an integrator:

$$\frac{dx}{dt} = K\varepsilon \quad \text{where } \varepsilon = \pm 1 \text{ and } K, \text{ a constant} \quad (2)$$

and a differentiator:

$$g = \frac{dy}{dt} \quad (3)$$

A logic circuitry subsystem is associated and implemented according to the following function:

- if $g < 0 \Rightarrow$ the sign of ε must change.
- if $g > 0 \Rightarrow$ the sign of ε keeps the same.

Fig. 5 explains the behaviour of the Extremum Seeking algorithm. Four cases can be distinguished.

Case 1: Vector a (a_x, a_y) describes a movement where both horizontal and vertical parts are increasing.

$$\left. \frac{dx}{dt} \right|_{t^-} > 0, \text{ and } \left. \frac{dy}{dt} \right|_{t^-} > 0.$$

Therefore, the controller must keep the sign of the horizontal variation.

$$\left. \frac{dx}{dt} \right|_{t^+} = K.$$

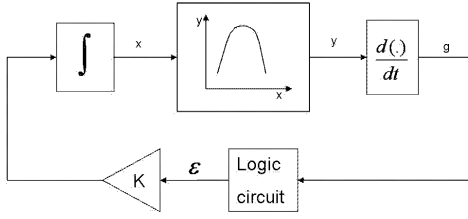


Fig. 4. Block diagram principle of Extremum Seeking Control.

Case 2: Vector b (b_x, b_y) describes a movement where the horizontal part is increasing while the vertical one is decreasing.

$$(dx/dt)|_{t^-} > 0, \text{ and } (dy/dt)|_{t^-} < 0.$$

Therefore, $(dx/dt)|_{t^+} = -K$.

Case 3: Vector c (c_x, c_y) describes a movement whose horizontal part is decreasing whereas its vertical one is increasing.

$$(dx/dt)|_{t^-} < 0, \text{ and } (dy/dt)|_{t^-} > 0.$$

Therefore, $(dx/dt)|_{t^+} = -K$.

Case 4: Vector d (d_x, d_y) describes a movement where both horizontal and vertical parts are decreasing.

$$(dx/dt)|_{t^-} < 0, \text{ and } (dy/dt)|_{t^-} < 0.$$

Therefore,

$$(dx/dt)|_{t^+} = K.$$

As $dy/dx = (dy/dt)/(dx/dt)$, then cases 1-4 can be expressed in compact form as following (4) and (5) equations:

$$\text{if } \frac{dy}{dx}|_{t^-} > 0 \quad \text{then} \quad \frac{dx}{dt}|_{t^+} = K \quad (4)$$

$$\text{if } \frac{dy}{dx}|_{t^-} < 0 \quad \text{then} \quad \frac{dx}{dt}|_{t^+} = -K \quad (5)$$

Equations (4) and (5) can also be reduced to only one expression below:

$$\frac{dx}{dt} = K \operatorname{sign}\left(\frac{dy}{dx}\right) \quad (6)$$

It can be notice that the algorithm evaluates the sign of dy/dt , whereas the resulting dynamics are dependent of dy/dx . Also, it can be observed in (6) that the equilibrium point $dx/dt=0$ corresponds to an Extremum of the $x-y$ curve (Fig.5), where $dy/dx=0$. In order to demonstrate that the equilibrium point is stable, a positive function $V(t)$ is defined in a concave domain of $y(x)$ like :

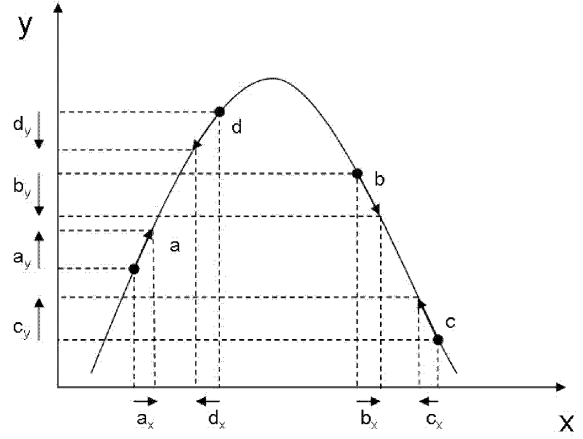


Fig. 5. Illustration of Extremum Seeking principle.

$$V(t) = \frac{1}{2} \left(\frac{dy}{dx} \right)^2 \quad (7)$$

Hence

$$\dot{V}(t) = \frac{dy}{dt} \frac{d^2y}{dx^2} \frac{dx}{dt} = \frac{dy}{dx} \frac{d^2y}{dx^2} \left(K \operatorname{sign}\left(\frac{dy}{dx}\right) \right) \quad (8)$$

The concavity of $y(x)$ can be translated by (9) and (10):

$$\frac{d^2y}{dx^2} < 0 \quad (9)$$

$$\frac{dy}{dx} \operatorname{sign}\left(\frac{dy}{dx}\right) > 0 \quad (10)$$

Therefore, choosing a positive value for K will imply:

$$\dot{V}(t) < 0.$$

As $V-P$ characteristics of a solar array are a concave function, the generic previous analysis can be applied to MPPT controllers.

The main difference between the MPPT of [4] and our MPPT is its digital processing (Fig 6). The tracking principle consists to increase or decrease the value of the PV voltage V_{pv} . Input parameters of the converter are imposed by the solar panel voltage and current (V_{pv}, I_{pv}). In this case, variables x and y of the Extremum Seeking Control principle (Fig.4 and Fig.5), must be substituted respectively by V_{pv} and the PV power P_{pv} such as $P_{pv} = V_{pv} \cdot I_{pv}$. The variation of V_{pv} through a constant time-derivate is achieved by imposing a particular behaviour of the converter duty cycle. The theoretical demonstration is exposed in [4]. The Extremum Seeking Control algorithm can be applied directly to the converter duty cycle which controls the power panel. In the example of the Fig.6, the load is a simple battery (v_B). The permanent search of the MPP is characterised by a voltage triangular waveform in the time-domain with slopes $-v_B$ and $+v_B$ respectively for the right to left and for the left to right movements, where is the converter duty cycle.

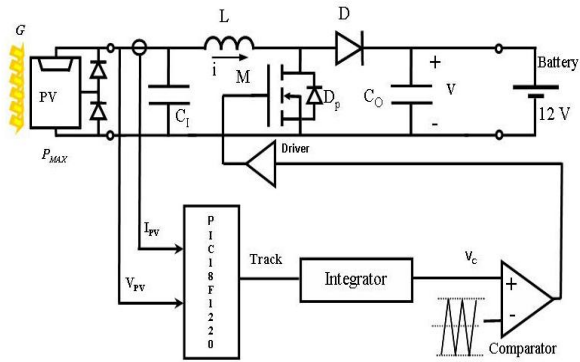


Fig. 6. Boost Converter + adaptive digital MPPT.

IV. DIGITAL MPPT ALGORITHM

For a great number of advantages (price, simplicity, reduction of size and components of the control circuit, flexibility, added functions,...), we chose to change the type of implementation control in a numerical one. Then, our Extremum Seeking algorithm was implemented in the PIC18F1220 microcontroller (Fig.6). Like in the previous versions, with only the measures of V_{pv} and I_{pv} , the control of the converter through its duty cycle allows to research and track the MPP when the PV is exposed to the climatic variation. The algorithm inserted inside the PIC is presented on Fig.7.

The intern Numerical Analogical Converter of PIC samples the measures of voltage and current values. With these acquisitions, a power image is established (P_{pv}) and compared with the previous one a time before (depending of step) named power (P_{pv-1}). This function of power comparison can be assimilated to a derivation of power.

If the result of this comparison is positive, the PV power point approaches the MPP, and if not, the system takes away the maximal power. In case of the derived power is positive, the *Track* signal keeps its value (as described in the section III), but inversely when the derived is negative theoretically, the *Track* signal state is changed. The *Track* signal is the output signal of microcontroller where the voltage is limited between 0 and 5V.

In the case of our numerical version, a function “delay” is added to the algorithm (symbolised by *H* variable in the algorithm, when the delay time is achieved $H=1$, otherwise $H=0$). This delay permits a certain stability of the system. Indeed, the *Track* signal value is maintained while the delay period is not finished.

The value of the delay depends of the time constant of the converter. This delay maintains the same progression to an MPP during several cycles of the algorithm. This function guarantees the stability of the converter at the time of the brutal variation of the sun radiation.

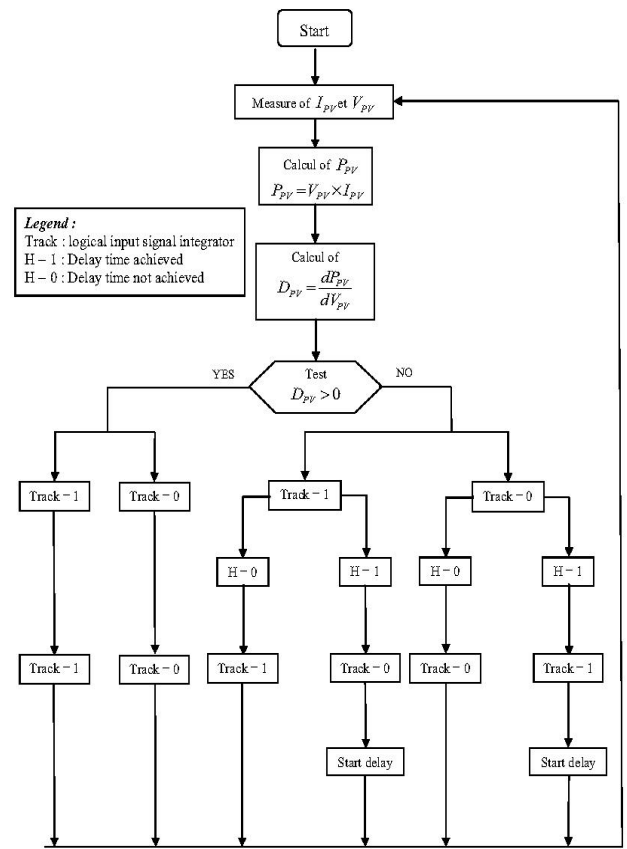


Fig. 7. MPPT algorithm.

In summarize:

- when the derived power is positive, the *Track* signal remains unchanged.
- when the derived is negative and the change authorized (delay finished), the *Track* signal state is modified.
- each *Track* signal inversion initialises the delay.

The block diagram of the algorithm is represented on Fig.8. The output signal of the microcontroller (*Track*) charges or discharges an integrator circuit. The output resulting signal constitutes the reference for the Pulse Width Modulation (PWM). This one is compared with a triangular waveform of a 230 kHz to generate the duty cycle of the converter.

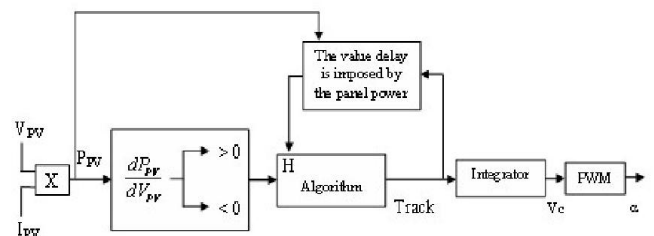
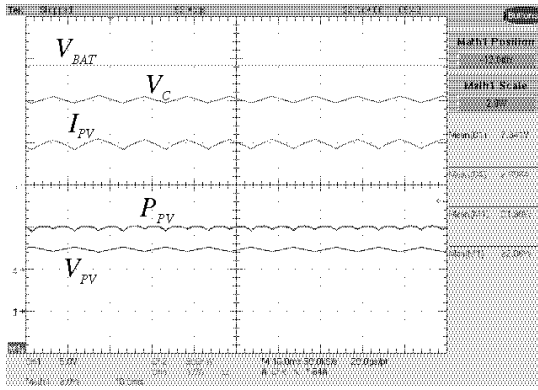
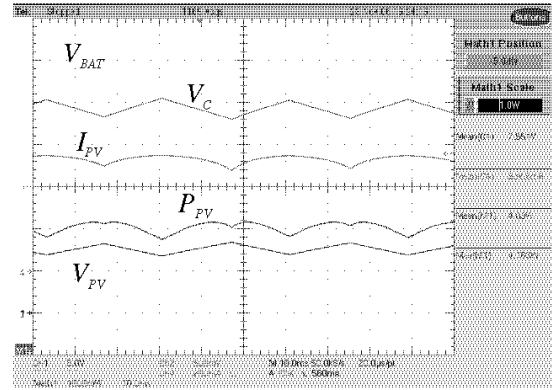


Fig. 8. Digital MPPT block diagram.



a) High power



b) Low power

Fig. 9. Steady state behaviour of PV array variables.

With our digital MPPT, we introduce a new aspect around the variation of the delay value. Indeed, the numerical implementation allows new possibilities in algorithms. In this context, to improve the matching of the MPPT tracking, we designed a new function to adapt the value of the delay H to the level of power transmitted. This new improvement allows a better efficiency at low powers without degrading performances at high power.

In one hand, a decreasing of delay time value H reduces the amplitude oscillation around the MPP and allows a better optimisation.

In the other hand at low power (low slope of $P_{PV}(V_{PV})$), the sampling noise generated on the acquisition signals induces difficulties to determinate the power derived. In consequence, the delay must be increasing to reach the MPP and to eliminate the noise effect. We propose a new function in our digital algorithm consisting to adapt the value of H according with the supply power. First experimental results are presented in the next part.

V. EXPERIMENTAL RESULTS

This section is focused on different examples of experimental results. The tests were realised with the prototype described in Fig.6 including the Boost converter and our adaptive digital MPPT. The input source is a solar panel (18 cells) of nominal power of 42W. The output source is constituted by a lead storage battery of nominal voltage of 12V.

A. Steady-state measurements.

Fig. 9 presents the research of the MPP when the system is submitted at a constant irradiation levels (high power Fig. 9(a), low power Fig. 9(b)) for our adaptive digital MPPT. These experimental results show that the PV MPPT control induces oscillations on the electrical signals. Nevertheless, we can show that ripples around the MPP of the PV array are different in form and amplitude. Indeed, the triangular waveform of the V_c control signal impose the variation of the duty cycle, which generates oscillations on the PV parameters depending on the form of $P(V)$ characteristics.

The negative slope of the V_c signal indicates that the operating point moves from the left to the right on the $P-V$ curve in direction of the MPP. With the positive slope, the direction is opposite. Then, during one period of V_c signal, the MPP is scanning two times. With this propriety, at each experimental statement, we can measure the value of the MPPT efficiency. This efficiency is obtained by the ratio between the PV extracted average power and the maximum power supply by the PV module. For Fig 9(a), the average power is 21.98W for a maximum power of 22.06W, given a MPPT efficiency of 99.6%. For Fig. 9(b), and an average power of 4.03 W, the MPPT efficiency reaches 96.8%, which allows a production of PV power even in low sun irradiation.

In the two cases, the maximum power point is obtained. In the two experimental tests the delay time is different, small for a high power and high for a low power. Today our digital control adjusts automatically the value delay according to the climatic conditions, to obtain the best conversion efficiency in high power. Also, our control guarantees a maximum power point tracking at low power keeping high conversion efficiency.

B. Comparative performance of our MPPT control.

To show the new interesting performance for adaptive digital MPPT we have realised three experimental results in same conditions with three MPPT versions (Fig. 10).

Fig.10 (a) corresponds to an analogical version [4], with a MPPT efficiency of $\eta_{MPPT} = 99.3\%$.

Fig.10 (b) is realised with a digital MPPT with H constant delay, performance can not really more optimised $\eta_{MPPT} = 99\%$.

Fig.10 (c) the experimental results have given with the adaptive digital MPPT a $\eta_{MPPT} = 99.4\%$. As shown in these examples ripples around electrical values are reduced in the case c.

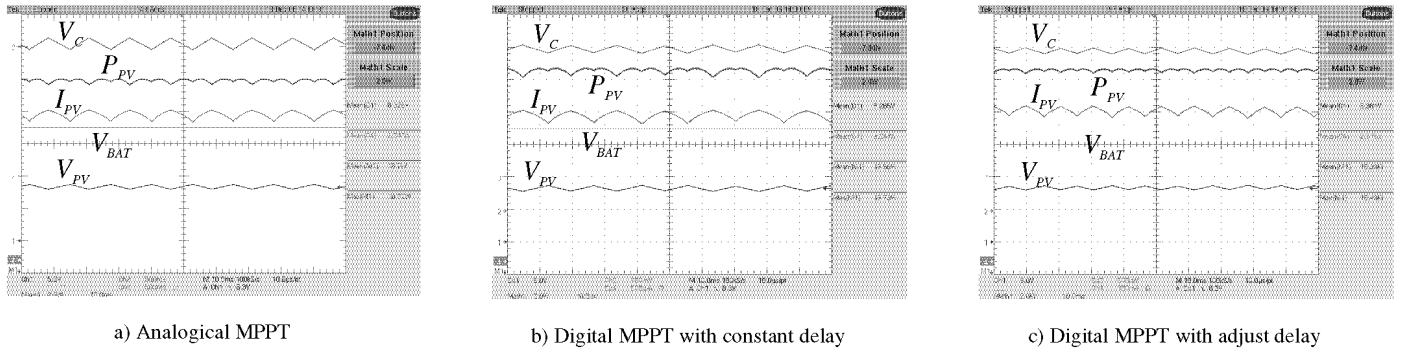


Fig. 10. Steady state behaviour of PV array variables.

C. Response of the system to different perturbations.

The addition test analyses the system behaviour when this one is exposed at brutal variations of the sun irradiation. Fig. 11 shows the behaviour of the PV electrical variables when occurs a brutal increasing of the sun radiation. In this type of change, the PV current increases immediately. The PV voltage remains practically unchanged and then the duty cycle remains identical allowing instantaneously a new recover of the MPP. The phenomenon is the same when the PV current decreases (low sun radiation). In this type of MPPT control, the losses of efficiency are minimised during transitory.

V. CONCLUSION

This paper has proposed a digital MPPT based on the Extremum Seeking Control with an H delay value adapting itself according to the level of P_{pv} . This system has a high efficiency in steady state but also during transitory. A small delay increases the efficiency conversion, a high delay guaranties to pass away the maximum power point. Compared with an analogical MPPT realised in the previous works, the digital control allows devising the consumption by four and reduce the number of components to obtain the same behaviour.

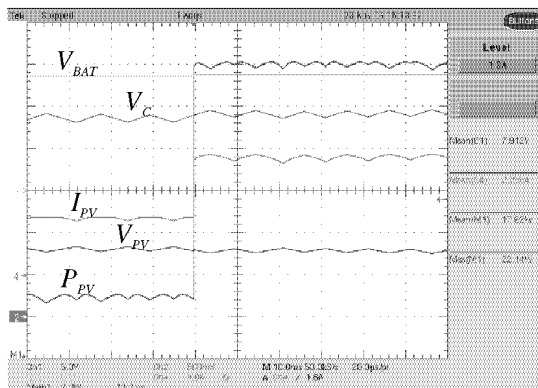


Fig. 11. Response of the system submitted to brutal increasing of solar radiation.

The digital control can be associated with other power converter structure and security function such as component temperature control, overcharging battery or alarm panel can be implemented. Those benefits contribute to have new PV systems with good conversion efficiencies and low prices.

VI. REFERENCES

- [1] T. Noguchi, D. Togashi, and R. Nakamoto, "Short-current pulsed-based maximum power point tracking method for multiple photovoltaic and converter module system," *IEEE Trans. Industrial Electronics*, vol. 49, Feb. 2002, pp. 217-223.
- [2] L. Dong-Yun, N. Hyeong-Ju, H. Dong-Seok, and C. Ick, "An Improved MPPT converter using current compensation method for small scaled PV-application," *IECON02*, vol. 2, Nov. 2002, pp. 1113-1118.
- [3] C. Alonso, M. F. Shraif, A. Martinez, CNRS patent, US 2005099166, "Power converter control for automatic maximum power point tracking".
- [4] R. Leyva, C. Alonso, and A. Cid-Pastor, "MPPT of photovoltaic System using Extremum-Seeking Control," *IEEE Aerospace and Electronic Systems*, vol. 42, Jan. 2006, pp. 249-258.
- [5] M. Veerachary, T. Senjyu, and K. Uezato, "Voltage-based maximum power point tracking control of PV system," *IEEE Aerospace and Electronic Systems*, vol. 38, Jan. 2002, pp. 262-270.
- [6] Y. Jung, J. So, G. Yu, and J. Choi, "Improved perturbation and observation method (IP&O) of MPPT control for photovoltaic power systems" *Photovoltaic Specialists Conference 2005*, Jan. 2005, pp. 1788-1791.
- [7] E. Koutroulis, K. Kalaitzakis, and N.C. Voulgaris, "Development of a microcontroller-based, photovoltaic maximum power point tracking control system" *IEEE Trans.*, vol 16, Jan. 2001, pp. 46-54.
- [8] A. Tariq, J. Asghar, "Development of a microcontroller-based maximum power point tracker for a photovoltaic panel" *Power India Conference 2006 IEEE*, Avr. 2006, 5 pp.
- [9] A. Cid Pastor, "Conception et realisation de modules photovoltaiques electronique", *Phd dissertation. Institut National des Sciences Appliquées de Toulouse, LAAS-CNRS Report Number 06688, Toulouse, France, Septembre 2006 (in French)Thesis of Paul Sabatier (Toulouse), 2006, LAAS report n° 06688.*